Ion and Electron Imaging Study of Isobutanal Photoionization Dynamics

Lei Shen, Prashant Chandra Singh, Myunghua Kim,[†] Bailin Zhang, and Arthur G. Suits*

Department of Chemistry, Wayne State University, Detroit, Michigan 48202

Received: September 5, 2008; Revised Manuscript Received: November 6, 2008

We present a detailed photoion and photoelectron imaging study of isobutanal cation dynamics. The 2 + 1 REMPI spectrum via the (n,3s) Rydberg transition was recorded and analyzed under both cold and warm beam conditions in an effort to identify the predicted trans conformer. Photoelectron imaging was used to establish the ion energetics accurately and to aid in the assignment of the REMPI spectra. On the basis of the photoelectron spectra and ab initio calculations, a peak at 54336.8 cm^{-1} is assigned to the trans conformer. We have also assigned the photoelectron spectra and identified some hot band transitions not reported in previous work. We determined the adiabatic ionization energy to be 9.738 eV. We also studied the photodissociation dynamics of isobutanal cations leading to several product channels, but no evidence of vibrational mode or conformational isomer dependence on either the product branching or dynamics was seen for this system.

Introduction

The conformational[1−4] and vibrational state selection[5] of polyatomic molecules and ions are of keen interest as a means of controlling unimolecular as well as bimolecular reaction dynamics[5−7] and probing features of the ground and excited-states of the potential energy surfaces of ionic systems. Two general strategies to prepare polyatomic cations with a well-characterized excitation in different vibrational modes or in different conformations are resonance-enhanced multiphoton ionization (REMPI)[8] and mass-analyzed threshold ionization (MATI)[9] techniques. In a simple REMPI scheme, the vibrational state or conformer selection in the cation can be achieved by resonant excitation to an intermediate Rydberg state followed by ionization by an additional photon. Further, the final ion internal state distribution can be determined from the photoelectron spectra measured for the REMPI transition through each intermediate level. In favorable cases, REMPI ionization will prepare single-ion vibrational and conformational states quite selectively, and these may be used for subsequent study of reaction or photodissociation dynamics. In other cases, such as those reported here, pure state preparation is not possible. Nevertheless, by measuring the photoelectron spectra, one may assign the REMPI spectrum with little ambiguity, and study photodissociation from a restricted range of excited vibrational levels of the cation.

Simple aliphatic aldehydes have been the subject of various experimental and theoretical studies,[10,11] both as model polyatomic systems and as one of the important intermediate species in isomerization reactions. Recently, our group has studied the conformers of propanal cation[12] and their photochemistry using ion and photoelectron imaging techniques. A surprising dependence of the dissociation dynamics on initial conformer was seen and interpreted on the basis of multisurface dynamical calculations. Another interesting molecule of this series is isobutanal (2-methyl propanal). Neutral isobutanal has two conformations: trans and gauche (see Figure 1). It has been
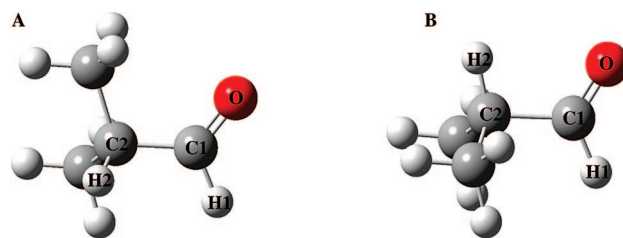

Figure 1. Optimized geometries for gauche (A) and trans (B) conformers of isobutanal cation at the B3LYP/6-311++G (d,p) level of theory.

shown that in the gas phase at room temperature, 90% of the molecules exist as the gauche conformer, while the remainder are in the trans form.[13] Various spectroscopic methods [14−18] ranging from microwave to infrared and UV have been applied to probe the isobutanal molecule potential energy surface over a broad wavelength range. These experiments confirmed that gauche and trans conformers of isobutanal are the only two minima on the potential energy surface. The gauche form is slightly more stable than the trans form, and the predicted energy difference is 250 ± 66 cm^{-1}.[18] Apart from this experimental study there are many theoretical studies[19,20] using various methods and basis sets that also concluded that the gauche form is more stable than the trans form in the ground state. In combined spectroscopic and ab initio study of isobutanal, Metha et al. reported that, for the ground state, the gauche form is 69 cm^{-1} more stable than the trans state, while, in the (n,3s) Rydberg state, the trans form is about 115 cm^{-1} lower in energy.[20] This study failed to identify any bands that could be associated with the trans form, however. In addition to these experimental studies, early photoelectron spectroscopy studies[21] found that the photoelectron spectrum of isobutanal was less intense than that of its straight chain analogue, and this was attributed to the many low-frequency vibrations that arise from a branched alkyl group.

The objectives of present study are (1) to expand and refine the REMPI spectra reported by Metha et al.[20] by complementing these with photoelectron imaging and varying beam conditions; (2) to employ high-resolution ion and photoelectron imaging[22,23]

* Corresponding author. E-mail: asuits@chem.wayne.edu
† Present address: Department of Chemistry, University of California, Santa Barbara, CA, 93106.

Electron Imaging Study of Isobutanal Cation Dynamics

J. Phys. Chem. A, Vol. 113, No. 1, 2009 **69**

TABLE 1: Optimized Geometrical Parameters and Energetics for the Gauche and Trans Conformers of the Isobutanal Cation at the B3LYP/6-311++G(d,p) Level of Theory

	ground state		cationic state	
	gauche	trans	gauche	trans
C1−C2 (pm)	151.6	151.5	165.9	161.9
C1−H1	111.4	111.6	110.9	110.8
C1=O	120.6	121.4	117.1	118.7
C2−H1	110.1	109.6	109.8	109.3
∠H2C2C1(°)	104.7	107.0	98.2	105.0
∠C2C1O	125.6	125.3	122.7	119.9
ΦH2C2C1H1	61.2	180.0	47.2	180.0
E_{B3LYP} (Hartree)	−232.531916	−232.531361	−232.178464	−232.180399
ΔE_{B3LYP} (cm^{-1})	121.80		424.68	
E_{G3} (Hartree)	−232.257500	−232.256569	−231.897200	−231.898389
ΔE_{G3} (cm^{-1})	204.33		260.95	

to determine the ionization energies and explore the conformational and vibrational state selectivity available in the cation ground electronic state prepared by a (2 + 1) REMPI scheme through the (n,3s) Rydberg state of isobutanal; and (3) to employ the results of these spectroscopic investigations to study photodissociation dynamics for state-selected isobutanal ions.

Experiment

The detailed description of our apparatus was reported elsewhere.[24] Isobutanal in the liquid phase is kept in a bubbler and seeded in the carrier gas at a backing pressure of ~3 atm. The gas mixture is introduced through a piezoelectric pulsed nozzle with a 1 mm orifice into the source chamber of our differentially pumped apparatus. After passing through the skimmer located 3.8 cm downstream of the pulsed valve, the supersonic molecular beam enters into the velocity mapping ion optics assembly consisting of four electrodes. The molecular beam is perpendicularly intersected with a laser beam tuned to a two-photon resonant excitation transition of the (n,3s) Rydberg state of isobutanal. The operating pressures are maintained at ~1.0×10^{-5} Torr in the source chamber and less than 5×10^{-8} Torr in the main chamber.

The laser beam is generated by the frequency doubling the output of a dye laser (Scanmate, LDS 722) pumped by the second harmonic of the Nd:YAG laser (Spectra-physics, GCR-5). The polarization of the laser is vertical, parallel to the surface of the detector, in order to monitor the electron angular distribution. The laser is focused with a lens (f = 30 cm) into the interaction volume. Typical output power of the laser beam is 1−2 mJ/pulse, and the wavelength calibration is achieved by a wavemeter (Coherent WaveMaster). Following ionization, the ions or electrons are accelerated through a multilens velocity mapping assembly. After passing through a field-free region, the particles impact upon a position sensitive dual MCP/P-47 Phosphor screen of 120 mm diameter (Burle) located 150 cm downstream from the interaction region (110 cm in the photoelectron experiment). During the photoelectron experiment, the inside of the chamber is shielded with a μ-metal sheet to avoid the influence of external magnetic fields. The resulting images are recorded by a CCD camera (Sony, XC-ST50) employing the IMACQ megapixel software,[25] developed in our group, which permits real-time event-counting and centroiding of the data. The three-dimensional (3-D) velocity distributions were reconstructed from the recording images using the basis set expansion (BASEX) program developed by Reisler and co-workers.[26] In order to obtain the standard photofragment kinetic energy release distributions, we perform two calibration experiments: one is Br_2[27] photodissociation ion imaging, and the other one is propanal photoelectron imaging.[28]

Results and Discussion

Theoretical Calculations. We have used ab initio methods to determine the geometries, energies and vibrational frequencies for gauche and trans conformers of isobutanal in both neutral and cationic states. All theses calculations have been performed by using Gaussian 03 software.[29] The structure of isobutanal was optimized at the B3LYP/6-311G++(d,p) level of theory, and the vibrational frequency of the optimized structure was calculated with the same level of theory to confirm the nature of the optimized structure on the potential energy surface. The optimized geometrical parameters of the neutral conformers are found to be in good agreement with the earlier report.[20] Figure 1 shows the optimized structures of the cationic isobutanal in the gauche (Figure 1a) and trans (Figure 1b) conformations. Table 1 shows the optimized parameters of the gauche and trans isomers of isobutanal in the ground and cationic states. In the cationic state, C1−C2, C1=O, ∠H2C2C1, and ∠C2C1O parameters change significantly as compared to the ground-state for both conformers, while the dihedral angle H2C2C1H1 changes only for the gauche conformer. Table 1 also depicts the electronic energy of both conformers calculated at the B3LYP/6-311++G(d,p) level of theory in the ground and cationic state. The B3LYP calculation shows that the ground-state gauche conformer is 121.8 cm^{-1} more stable than the trans conformer, which is consistent with the earlier reported value in the literature,[20] while in the cation, the trans form was found to be 424.7 cm^{-1} more stable than the gauche cation. It is well-known that the B3LYP method is not an entirely reliable method to get the accurate energetics, as it does not account for the dispersion energy contribution. To get more accurate energetics of the two conformers, a G3 calculation was performed, and the results are tabulated in Table 1. The G3 calculation follows the same energetic trend as B3LYP, and shows that the gauche conformer is 204.3 cm^{-1} more stable than the trans conformer in the ground-state, while the trans conformer is 260.9 cm^{-1} more stable in the cationic state. The unscaled calculated vibrational frequencies of the cationic isobutanal conformers at B3LYP/6-311++G (d,p) have been depicted in Table 2. It is observed that the most significant differences between the ground-state and cationic-state frequencies are in the C2C1 stretch (ν_{14}), C2C1O bend (ν_{16}), C2H bend (ν_{11}), aldehydic CH bend (ν_{10}) and C=O stretch (ν_6). These frequency changes are quite similar to those reported by Metha et al. for isobutanal between the ground and excited states.

REMPI Spectra. The jet-cooled (2 + 1) REMPI spectrum of isobutanal recorded at m/z = 43 was already reported by Mehta et al.,[20] and they assigned all the observed vibronic transitions as arising from the vibrationless gauche conformer.

TABLE 2: Calculated Unscaled Vibrational Frequencies (cm^{-1}) for the Gauche and Trans Conformers of Isobutanal Cation at B3LYP/6-311++G (d,p) Level of Theory

	vibrational mode	assignment	vibrational frequency/cm^{-1}	
			gauche	trans
a′	C2H2 stretch	ν_1^+	3025.8	3110.9
	CH$_3$ antisymmetric stretch	ν_2^+	3139.6	3129.6
	CH$_3$ antisymmetric stretch	ν_3^+	3094.4	3083.3
	CH$_3$ symmetric stretch	ν_4^+	3013.2	3000.4
	aldyhydic CH stretch	ν_5^+	2900.7	2932.7
	C=O stretch	ν_6^+	1833.9	1806.1
	CH$_3$ antisymmetric deformation	ν_7^+	1499.3	1498.7
	CH$_3$ antisymmetric deformation	ν_8^+	1473.3	1436.2
	CH$_3$ symmetric deformation	ν_9^+	1447.3	1396.7
	aldehydic CH bend	ν_{10}^+	1034.9	1127.3
	C2H2 bend	ν_{11}^+	1230.8	1227.2
	CH$_3$ rock	ν_{12}^+	1187.8	1176.4
	CH$_3$ rock	ν_{13}^+	1002.5	1010.7
	C2C1 stretch	ν_{14}^+	438.3	414.7
	C4C2C3 symmetric stretch	ν_{15}^+	821.3	826.0
	C2C1O bend	ν_{16}^+	483.5	557.7
	C2C2 wag	ν_{17}^+	374.7	352.4
	C2C2 deformation	ν_{18}^+	305.4	283.5
	CH$_3$ torsion	ν_{19}^+	239.6	237.6
a″	CH$_3$ antisymmetric stretch	ν_{20}^+	3132.2	3135.6
	CH$_3$ antisymmetric stretch	ν_{21}^+	3083.7	3081.8
	CH$_3$ symmetric stretch	ν_{22}^+	2987.8	2988.7
	CH$_3$ antisymmetric deformation	ν_{23}^+	1499.3	1475.6
	CH$_3$ antisymmetric deformation	ν_{24}^+	1425.7	1420.9
	CH$_3$ symmetric deformation	ν_{25}^+	1375.6	1372.6
	C2H2 bend	ν_{26}^+	1340.0	1337.6
	C4C2C3 antisymmetric stretch	ν_{27}^+	1089.9	1041.2
	CH$_3$ rock	ν_{28}^+	943.9	949.9
	CH$_3$ rock	ν_{29}^+	898.9	902.8
	aldehydic CH bend	ν_{30}^+	858.1	881.6
	C2C2 twist	ν_{31}^+	374.7	305.3
	CH$_3$ torsion	ν_{32}^+	204.7	211.2
	formyl torsion	ν_{33}^+	58.9	95.3

The band at 53495.0 cm^{-1} was attributed to the gauche−gauche origin transition, and their attempt to find the trans−trans origin was unsuccessful. In order to get additional insight into this system, we recorded (2 + 1) REMPI spectra of isobutanal at $m/z = 43$ under various conditions, changing the backing pressure and the carrier gas. Trace A in Figure 2 shows the (2 + 1) REMPI spectrum of isobutanal in cold conditions (300 KPa Argon), while Trace B shows the spectrum in relatively
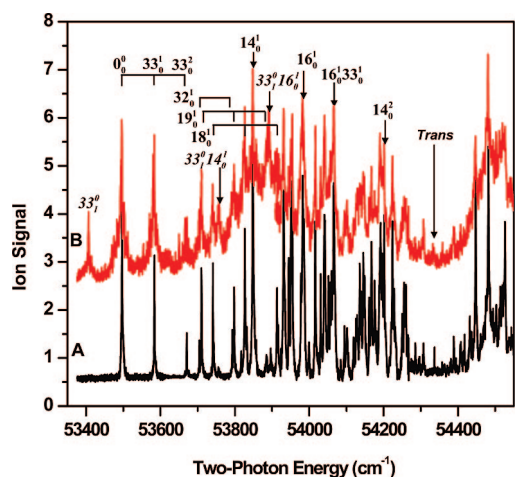

Figure 2. The one-color (2 + 1) REMPI of isobutanal recorded at $m/z = 43$ in different beam conditions. Trace A is the jet-cooled spectrum (300 KPa Argon), while Trace B is recorded in hot conditions (without carrier gas). Trace B is offset for clarity. The peaks marked in italics are new or revised assignments. The combs show formyl torsion progressions (mode 33).

hot conditions (without carrier gas). The cold spectrum is in very good agreement with the earlier report,[20] but, in contrast to this, the hot spectrum has several new features. In the hot beam spectrum, the gauche origin appearing at 53495 cm^{-1}, has a short progression of formyl torsion with 88 cm^{-1} energy interval, as seen in the cold spectra reported here and earlier.[20] The first new peak in the hot spectrum was found to be ∼88 cm^{-1} to the red of the gauche band origin, and can readily be assigned to a hot band of formyl torsion. Other new features in the warm spectrum were found at 53758.4, 53896, and 53999.8 cm^{-1}. The peak at 53758.4 cm^{-1} is ∼90 cm^{-1} red-shifted from the 14_0^1 transition and is temperature-dependent and broad, leading to assignment as the $33_1^0 14_0^1$ transition. The peak at 53896 is 85.7 cm^{-1} away from the 16_0^1 transition, and its temperature dependence leads to assignment as the $33_1^0 16_0^1$ transition. The peak at 53999.8 cm^{-1} is assigned to the $18_0^1 33_0^2$ transition, and the peak at 53977.9 cm^{-1}, which was also found in the cold beam and has not been assigned previously, is assigned as the 18_0^2 transition. The peak at the 54336.8 cm^{-1}, which is present in both beam conditions, was assigned to the $14_0^1 16_0^1$ transition by Metha et al.[20] We assign this peak to the trans−trans origin as discussed further below.

Photoelectron Spectra. Recently, our group has studied photoelectron imaging and photodissociation dynamics for different conformers of propanal cation and found it to be a powerful tool to aid in the spectral assignment.[28] Figure 3 shows the photoelectron images and corresponding photoelectron spectra measured by the one-color (2 + 1) REMPI of isobutanal for the gauche band origin 0_0^0, and the 33_0^1, 33_0^2, 14_0^1, and 14_0^2 transitions. The electron kinetic energy release spectra were obtained from the images, and most of them show a progression of three peaks. The strongest peak in the photoelectron spectrum of the gauche band origin transition (shown in Figure 3A), with 0.212 eV electron kinetic energy release, corresponds to the vertical (Franck−Condon diagonal favorable, $\Delta\nu = 0$) transition. The adiabatic ionization energy for the gauche conformer is then determined to be 9.738 eV, which is in reasonable agreement with the earlier report of 9.69 eV. The next two peaks are found 427 and 843 cm^{-1} from the vibrationless ground-state of the gauche isobutanal cation, i.e., a progression of about 420 cm^{-1}. This is close to the frequency calculated for the ν_{14}^+ vibration, 438.3 cm^{-1} (shown in Table 2), so these peaks are assigned to a progression in ν_{14}^+, the C1C2 stretch mode. This is based both on the agreement with the calculated frequency and the dramatic change in this frequency from the neutral (1000 cm^{-1}) to the ion, consistent with the activation of the C1C2 stretch upon photoabsorption. Durig et al. has also reported the same structural difference between the ground and Rydberg state, which also supports this assignment.[19]

Figure 3B,C shows the photoelectron images and spectra of the 33_0^1 and 33_0^2 transitions, which show a similar progression as the gauche origin transition. These spectra also have two members of the mode 14 progression, as well as a vertical ionization transition from the Rydberg level in these two transitions. Figure 3D,E shows photoelectron images and spectra of the 14_0^1 and 14_0^2 transitions. The 14_0^1 spectrum has a dominant peak at 0.229 eV, which can be readily assigned to the vertical transition by considering the energy of the ν_{14}^+ modes. The first peak, which is ∼400 cm^{-1} higher in energy than the main peak, is thus attributed to the vibrationless gauche cation. Similarly, in the photoelectron spectra of 14_0^2, the intense peak at 0.264 eV is assigned to the vertical ionization to two quanta in ν_{14}^+. There is a small feature at 0.364 eV that is assigned to the production of the vibrationless parent ion. Above all, these

Electron Imaging Study of Isobutanal Cation Dynamics

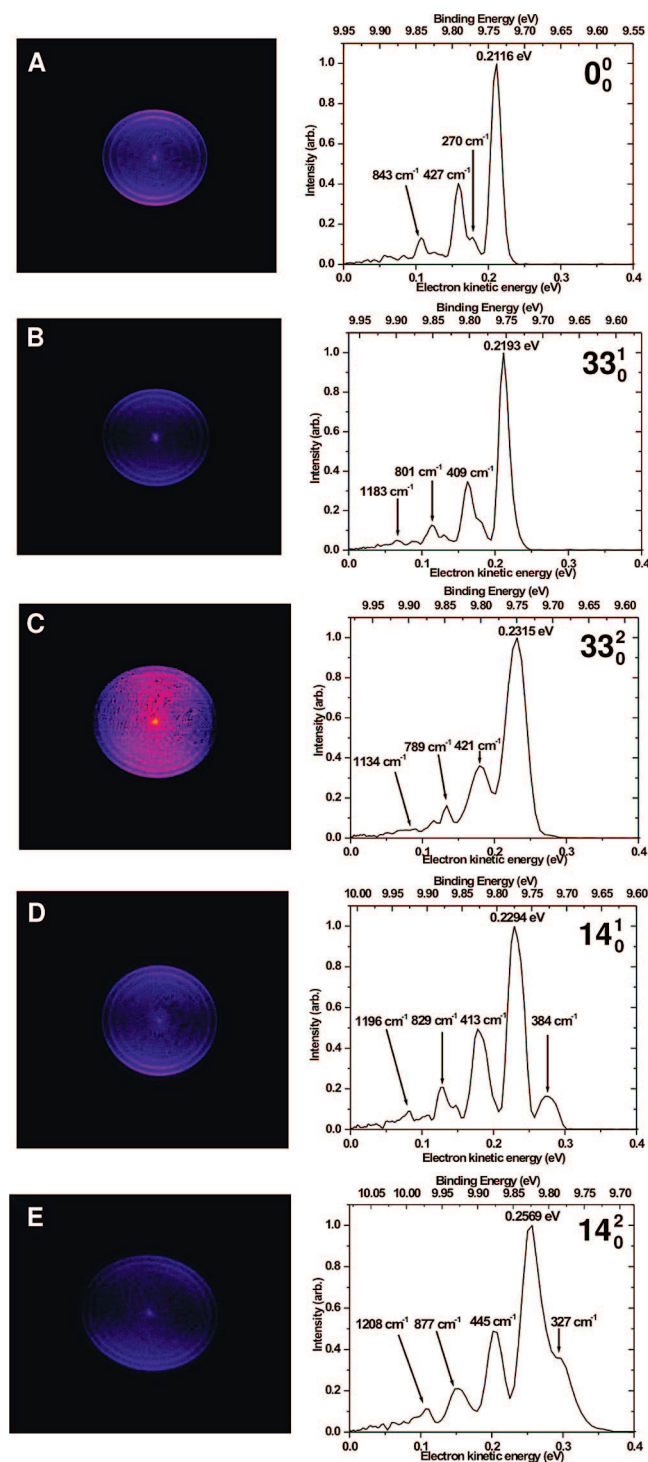*J. Phys. Chem. A, Vol. 113, No. 1, 2009* **71**

Figure 3. Photoelectron images and photoelectron kinetic energy distributions measured by one-color $(2 + 1)$ REMPI of isobutanal via (A) 0_0^0 gauche band origin (53495 cm^{-1}), (B) 33_0^1 (53583.8 cm^{-1}), (C) 33_0^2 (53671.0 cm^{-1}), (D) 14_0^1 (53848.6 cm^{-1}), and (E) 14_0^2 (54201.5 cm^{-1}) transitions.

photoelectron spectra are dominated by the ν_{14} mode progression. These facts clearly indicate that C1C2 is an active vibration mode of this REMPI transition, and the C1C2 bond length must be different in the ground and cationic state. We have also recorded the photoelectron spectra of the other transitions: 16_0^1, $16_0^1 33_0^1$. The images and photoelectron spectra of 16_0^1 and $16_0^1 33_0^1$ all show primarily Franck–Condon diagonal ionization with at least three members of the ν_{14} progression. Table 3 shows all the assignments of the photoelectron spectra obtained from the $(2 + 1)$ REMPI transitions for isobutanal.

TABLE 3: Assignments of the Photoelectron Spectra Obtained from $(2 + 1)$ REMPI Transitions for Isobutanal via the 3s Rydberg State

	0_0^0	33_0^1	33_0^2	$33_1^0 14_0^1$	14_0^1	$33_0^0 16_0^1$	16_0^1	14_0^2
0	0	0	0	0	0	0	0	0
ν_{33}^+		70						
$2\nu_{33}^+$			160					
ν_{14}^+	427	409	421	410	385	390		395
$2\nu_{14}^+$	843	801	789	827	799	814		799
$3\nu_{14}^+$		1183	1134	1215	1215			1244
$4\nu_{14}^+$				1584	1582			1676
$5\nu_{14}^+$								2007
ν_{16}^+							439	
$2\nu_{16}^+$							864	
$3\nu_{16}^+$							1255	
$4\nu_{16}^+$								

The Trans Conformer. Photoelectron imaging of the peak at 54336.8 cm^{-1} has also been recorded and is shown in Figure 4. The photoelectron spectrum of this transition is totally different from all other peaks, with the fundamental transition appearing at 0.420 eV, while the most intense transition is observed at 0.270 eV. The separation between these two peaks is ~1200 cm^{-1}, which is more than the combination of ν_{14} with ν_{16} and rules out the possibility of $14_0^1 16_0^1$, assigned by Metha et al.[20] From the experimental ionization energy of the gauche conformer, the electron kinetic energy release anticipated if this were the gauche conformer is estimated to be 0.366 eV. However, the spectrum has no feature at this kinetic energy release, arguing against the possibility of its assignment as the gauche conformer or its $14_0^1 16_0^1$ vibrational mode. The higher electron kinetic release clearly indicates that it belongs to a species that has lower energy than the gauche conformer in the
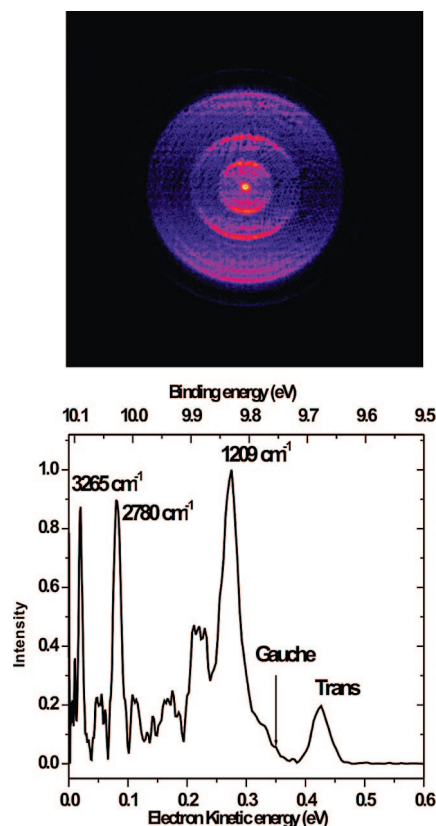

Figure 4. Photoelectron image and photoelectron kinetic energy distribution measured by one-color $(2 + 1)$ REMPI of isobutanal at 54336.8 cm^{-1}, assigned as the trans conformer origin.

cationic state. As mentioned above, the G3 calculation shows that trans is 260.9 cm^{-1} more stable than the gauche conformer in the cationic state. This leads us to assign this transition to the trans conformer. In one of the earlier studies of isobutanal, the trans−trans origin transition was calculated at the CIS level to lie ∼140 cm^{-1} to the red of the gauche−gauche origin, but they could never find the trans−trans origin experimentally.[20] However, in our observation, even in the warmest beam conditions, apart from the hot band of formyl torsion, nothing is detected to the red of the gauche band origin. Several new transitions have appeared to the blue of the gauche−gauche origin in the warm spectrum of isobutanal, and their temperature dependence implies that all of them are hot bands. To obtain more insight for assignment of this photoelectron spectrum, the ionization energy of the trans isobutanal was calculated. On the basis of the G3 calculated energetic difference between the two conformers of isobutanal in the neutral state (204.3 cm^{-1}) and the ionic state (260.9 cm^{-1}), the ionization energy of the trans conformer is calculated to be 9.68 eV, which implies the peak position of the vibrationless ion level of the trans conformer to be about 0.421 eV. This calculated value is in close agreement with the peak at the 0.420 eV electron kinetic energy release, strongly supporting this assignment as the vibrationless level of the trans cation. The photoelectron spectra and ab initio calculations thus give strong evidence for the assignment of the peak at 54336.8 cm^{-1} in the REMPI spectrum as the trans origin. In the photoelectron spectrum, the next intense peak, which has 1209 cm^{-1} internal energy relative to the trans origin, matches with the 1227.2 cm^{-1} ab initio frequency for one quantum of the ν_{11}^+ (C2H2 bend), and can thus be assigned as $\nu_{11}^+ = 1$ of the trans conformer cation. The next four features of lower intensity are spaced by ∼400 cm^{-1} and can be assigned as one, two, three, and four quanta of the ν_{14}^+ mode combined with one quantum in the ν_{11}^+ mode. The second intense peak at 2780 cm^{-1} from the trans origin can be assigned as a combination of $\nu_6^+ + \nu_{10}^+$ (∼2758 cm^{-1}). This assignment is justified, as there is large frequency change in the C=O stretch and aldehydic CH bend upon ionization from trans neutral to the cationic state. The last intense peak is 3265 cm^{-1} from the main vibrationless peak and can be assigned as a combination of $\nu_6^+ + \nu_{10}^+ + \nu_{14}^+$ (3270 cm^{-1}), as they are all the active modes for the transition.

Photodissociation. Although the photoelectron spectra show that in this case we are limited in our ability to prepare pure cation vibrational levels, in general they suggest fairly clean diagonal ionization from the Rydberg level on which a low-frequency progression is consistently superimposed. Subsequent photofragmentation of these REMPI-produced isobutanal cation takes place following absorption of an additional photon. In what follows, we have assumed that dissociation occurs following absorption of a single additional photon by the cation. These experiments are performed at relatively low laser power, so this assumption is not unreasonable. Furthermore, in the translational energy distributions, we find no evidence of energies beyond that permitted for a single photon abosrption. However, the possibility of multiphon processes in the cation are not ruled out by these results.

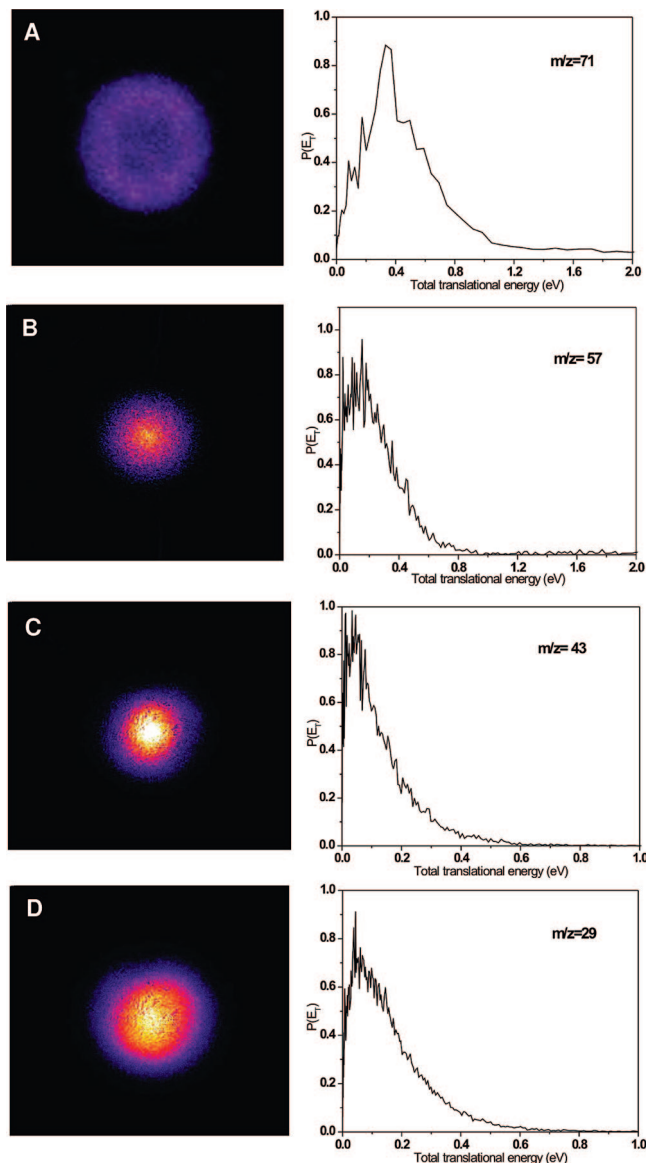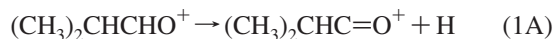There are four main channels for the photodissociation processes of isobutanal:

$$(CH_3)_2CHCHO^+ \rightarrow (CH_3)_2CHC=O^+ + H \quad (1A)$$

$$(CH_3)_2CHCHO^+ \rightarrow (CH_3)CH_2CCHOH^+ + H \quad (1B)$$

$$(CH_3)_2CHCHO^+ \rightarrow (CH_3)CHCHO^+ + CH_3 \quad (2)$$

Figure 5. Ion mages of different dissociation channels and respective total translational energy distributions following excitation on the 0_0^0 gauche transition.

$$(CH_3)_2CHCHO^+ \rightarrow (CH_3)_2CH^+ + CHO \quad (3)$$

$$(CH_3)_2CHCHO^+ \rightarrow CHO^+ + (CH_3)_2CH \quad (4)$$
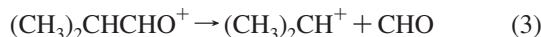
The resulting masses of the photofragment ions are 71, 57, 43, and 29, respectively. From the signal of theses masses, we find that mass 43 is the most intense, showing the loss of 29 amu. The signal intensity of masses 29 (channel 4), 57 (channel 2), and 71 (channel 1) decrease in this order. Figure 5 depicts the images and translational energy distributions obtained from the dissociation of isobutanal cation in all four channels. The angular distribution of the fragments is isotropic, which likely implies long lifetimes prior to dissociation. Except for the H loss image (channel 1), the translational energy distributions all peak at low energy, also implying statistical unimolecular decay.

The image for channel 1 dissociation has a hole in the central part of the image, which is also consistent with statistical decay, albeit with subsequent secondary decomposition that depletes some portion of the products with the highest internal energy. For the hydrogen elimination photoproduct at $m/z = 71$ there
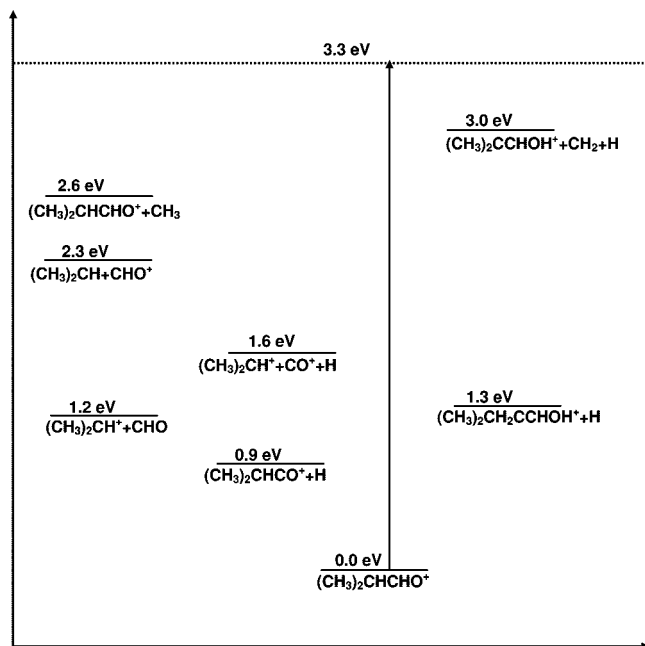
Electron Imaging Study of Isobutanal Cation Dynamics

J. Phys. Chem. A, Vol. 113, No. 1, 2009 **73**

Figure 6. Energy level diagram for key products of isobutanal cation dissociation relative to the cation ground state. The nominal excitation energy is shown as a dashed line.

TABLE 4: Total Available Energy and Average Translational Energy Values for Dissociation Channels 3 and 4 Obtained from Image Analysis

excitation wavelength	vibrational state of ions	E_{avail} (eV)		$\langle E_T \rangle$ (eV)	
		$m/z = 43$	$m/z = 29$	$m/z = 43$	$m/z = 29$
373.87	0_0^0	2.13	0.99	0.20	0.16
372.37	19_0^1	2.14	1.01	0.19	0.14
370.50	16_0^0	2.16	1.03	0.17	0.14
369.92	$16_0^0 33_0^1$	2.16	1.03	0.20	0.15
369.00	14_0^1	2.17	1.04	0.18	0.14

the remaining 85% in internal degrees of freedom. This is also consistent with the aforementioned two-step mechanism dominating the production of the former ion. Despite a thorough investigation, we found no evidence of vibrational mode dependence on either the product branching or dynamics for this system.

Conclusion

We have studied the detailed photoionization dynamics and spectroscopy of isobutanal and the phoodissociation dynamics of the cation using REMPI combined with photoelectron and photoion imaging. The (2 + 1) REMPI spectrum has been recorded under both cold and warm beam conditions to aid in assigning the spectra and to identify the "missing" trans conformer. The REMPI spectrum in the warm beam showed several new features that have been assigned to hot bands associated with various low-frequency transitions. The photoelectron spectra of almost all peaks are similar and dominated by the v_{14} mode progression. Interestingly, the photoelectron spectra of the peak at 54336.8 cm^{-1} was different from all others. To gain more insight into these photoelectron spectra, ab initio calculations were performed for the gauche and trans conformers in both ground and ionic states. The energetic calculation and photoelectron spectrum has unambiguously supported assignment of the 54336.8 cm^{-1} transition to the trans conformer. The photoelectron imaging results not only help the assignment of the REMPI spectra but also give the adiabatic ionization energy of isobutanal in the two conformations. Ion imaging results have shown that there are several decompositon pathways in the photodissociation process. The dynamics were interpreted on the basis of the translational energy distributions and known thermochemistry, but no evidence of vibrational mode or conformational isomer dependence on either the product branching or dynamics was observed in this system.

References and Notes

(1) Park, S. T.; Kim, S. K.; Kim, M. S. *Nature* **2002**, *415*, 306.
(2) Khriachtchev, L.; Macoas, E.; Pettersson, M.; Rasanen, M. *J. Am. Chem. Soc.* **2002**, *124*, 10994.
(3) Martinez-Nunez, E.; Bazquez, S. A.; I; Borges, J.; Rocha, A. B.; Estevez, C. M.; Castillo, J. F.; Aoiz, F. J *J. Phys. Chem. A* **2005**, *109*, 2836.
(4) Shemesh, D.; Gerber, R. B *J. Chem. Phys.* **2005**, *122*, 241104/1.
(5) Crim, F. F. *J. Phys. Chem.* **1996**, *100*, 12725.
(6) Anderson, S. L. *Acc. Chem. Res.* **1997**, *30*, 28.
(7) Green, R. J.; Anderson, S. L. *Int. Rev. Phys. Chem.* **2001**, *20*, 165.
(8) Anderson, S. L. *Adv. Chem. Phys.* **1992**, *82*, 177.
(9) Schlag, E. W. *ZEKE Spectroscopy*; Cambridge University Press: Cambridge, 1998; p 112.
(10) Buntine, M. A.; Metha, G. F.; McGilvery, D. C.; Morrison, R. J. S. *J. Mol. Spectrosc.* **1994**, *165*, 12.
(11) Metha, G. F.; Buntine, M. A.; McGilvery, D. C.; Morrison, R. J. S. *J. Mol. Spectrosc.* **1994**, *165*, 32.

are several stable isomers, of which (CH$_3$)$_2$CHC=O$^+$ (channel 1A) and (CH$_3$)CH$_2$CCHOH$^+$ (channel 1B) with the total available energy of 2.4 and 2.0 eV, respectively, are in reach of the UV photon (see Figure 6). For the former species, the threshold for CO loss is only 0.7 eV. This implies that any (CH$_3$)$_2$CHC=O$^+$ formed with translational energies below 1.7 eV will not be stable, instead undergoing dissociation, (CH$_3$)$_2$CHC=O$^+$ → (CH$_3$)$_2$CH$^+$ + CO. However, all of our m/z = 71 product is found at translational energies between ∼0.1 and 1 eV. For the other possible H loss product, the secondary fragmentation (CH$_3$)CH$_2$CCHOH$^+$ → (CH$_3$)CCHOH$^+$ + CH$_2$ has a threshold at 3 eV relative to the parent ion, or at a translational energy of 0.3 eV or below in our experiment. This is consistent with the m/z = 71 data in Figure 5A, so we assign all the observed m/z = 71 to the latter process, channel 1B. Does this mean that there is no H loss to give (CH$_3$)$_2$CHC=O$^+$? On the contrary, it suggests that any of this product formed at translational energies of 1.7 eV or below will necessarily lose CO to give m/z = 43, which is in fact the dominant ion. The absence of significant m/z = 71 signal at translational energies higher than 1.7 eV implies that all (CH$_3$)$_2$CHC=O$^+$ product must undergo secondary decomposition. The bulk of the m/z = 43 is thus likely the result of this two-step process involving channel 1A rather than direct HCO loss (channel 3). Recently, we observed distinct photodissociation behavior for the hydrogen atom elimination from propanal cation for the two analogous channels, depending on the starting conformer.[12] Our results here are reminiscent of the behavior of the *cis*-propanal cation, which was dominated by the formation of the hydroxyallyl isomer following H elimination.

The potential energy diagram for the possible channels within our 3.3 eV photon energy is depicted in Figure 6. Table 4 summarizes the available and average translational energy release data for the dissociation process of channels 3 and 4. The (CH$_3$)$_2$CH$^+$ ion produced has 9% of its total available energy as translational energy, with the remaining 91% in internal excitation. Similarly, for HCO$^+$ (produced in channel 4) there is 15% of the total available energy in translation with

(12) Kim, M. H.; Shen, L.; Tao, H. L.; Martinez, T. J.; Suits, A. G. *Science* **2007**, *315*, 1561.

(13) Guillory, J. P.; Bartell, L. S. *J. Chem. Phys.* **1965**, *43*, 654.

(14) Lucazeau, G.; Sandorfy, C. *J. Mol. Spectrosc.* **1970**, *35*, 214.

(15) Robin, M. B. *Higher Excited States of Polyatomic Molecules*; Academic Press: New York, 1975; Vol. II.

(16) Stiefvater, O. L. *Z. Naturforsch. A* **1986**, *41*, 483.

(17) Stiefvater, O. L. *Z. Naturforsch. A* **1986**, *41*, 641.

(18) Durig, J. R.; Guirgis, G. A.; Little, T. S.; Stiefvater, O. L. *J. Chem. Phys.* **1989**, *91*, 738.

(19) Durig, J. R.; Guirgis, G. A.; Brewer, W. E.; Little, T. S. *J. Mol. Struct.* **1991**, *248*, 49.

(20) Metha, G. F.; Buntine, M. A.; Bradley, A. J.; Morrison, R. J. S. *J. Mol. Spectrosc.* **2001**, *206*, 73.

(21) Tam, W.; Lee, D.; Brion, C. E. *J. Electron Spectrosc.* **1974**, *4*, 77.

(22) Chandler, D. W.; Houston, P. L. *J. Chem. Phys.* **1987**, *87*, 1445.

(23) Eppink, A.; Parker, D. H. *Rev. Sci. Instrum.* **1997**, *68*, 3477.

(24) Leskiw, B. D.; Kim, M. H.; Hall, G. E.; Suits, A. G. *Rev. Sci. Instrum.* **2005**, *76*, 104101.

(25) Li, W.; Chambreau, S. D.; Lahankar, S. A.; Suits, A. G. *Rev. Sci. Instrum.* **2005**, *76*, 063106.

(26) Dribinski, V.; Ossadtchi, A.; Mandelshtam, V. A.; Reisler, H. *Rev. Sci. Instrum.* **2002**, *73*, 2634.

(27) Vieuxmaire, O. P. J.; Nix, M. G. D.; Fitzpatrick, J. A. J.; Beckert, M.; Dixon, R. N.; Ashfold, M. N. R. *Phys. Chem. Chem. Phys.* **2004**, *6*, 543.

(28) Kim, M. H.; Shen, L.; Suits, A. G. *Phys. Chem. Chem. Phys.* **2006**, *8*, 2933.

(29) Frisch, M. J. Trucks, G. W.; Schlegel, H. B.; Scuseria, G. E.; Robb, M. A.; Cheeseman, J. R.; Montgomery, J. A., Jr.; Vreven, T.; Kudin, K. N.; Burant, J. C.; Millam, J. M.; Iyengar, S. S.; Tomasi, J. Barone, V.; Mennucci, B.; Cossi, M.; Scalmani, G.; Rega, N.; Petersson, G. A.; Nakatsuji, H.; Hada, M.; Ehara, M.; Toyota, K.; Fukuda, R.; Hasegawa, J.; Ishida, M.; Nakajima, T.; Honda, Y.; Kitao, O.; Nakai, H.; Klene, M.; Li, X.; Knox, J. E.; Hratchian, H. P.; Cross, J. B.; Adamo, C.; Jaramillo, J.; Gomperts, R.; Stratmann, R. E.; O. Yazyev; Austin, A. J.; Cammi, R.; Pomelli, C.; Ochterski, J. W.; Ayala, P. Y.; Morokuma, K.; Voth, G. A.; Salvador, P.; Dannenberg, J. J.; Zakrzewski, V. G.; Dapprich, S.; Daniels, A. D.; Strain, M. C.; Farkas, O.; Malick, D. K.; Rabuck, A. D.; Raghavachari, K.; Foresman, J. B.; Ortiz, J. V.; Cui, Q.; Baboul, A. G.; Clifford, S.; Cioslowski, J.; Stefanov, B. B.; Liu, G.; Liashenko, A.; Piskorz, P.; Komaromi, I.; Martin, R. L.; Fox, D. J.; Keith, T.; Al-Laham, M. A.; Peng, C. Y.; Nanayakkara, A.; Challacombe, M.; Gill, P. M. W.; Johnson, B.; Chen, W.; Wong, M. W.; Gonzalez, C.; Pople, J. A. *Gaussian 03*, revision B.03; Gaussian, Inc.: Pittsburgh, PA, 2003.